Int J Theor Phys (2011) 50: 181–199
DOI 10.1007/s10773-010-0507-y

Nonclassical Properties of Squeezed Finite-Dimensional Pair Coherent State

M. Sebawe Abdalla · A.S.-F. Obada · M. Darwish

Received: 12 May 2010 / Accepted: 20 September 2010 / Published online: 9 October 2010

Abstract We study the effect of the squeeze operator on the finite pair-coherent state. The state is a type of a correlated two-mode state in finite dimension based on the resonant ion-cavity interaction. We have discussed some statistical properties for such state, especially the quadrature variances as well as the second-order correlation function. Furthermore we have also considered the variance in the photon number sum and difference in addition to the linear correlation function. It is shown that the strong correlation occurs for a large value of the photon number difference. Our discussion is extended to include the quasiprobability distribution functions (W-Wigner and Q-functions). In the meantime we have considered the quadrature distribution function and phase distribution. It has been shown that the squeezed finite pair coherent state is sensitive to the variation in the state parameter, ξ and the squeeze parameter, r, as well as the q parameter which in fact plays a crucial role of controlling the behavior of the system.

Keywords Nonclassical state · Squeezing phenomenon · Quasi distribution functions

1 Introduction

Recently a new nonclassical state of electromagnetic field was generated by using the competition of four-wave mixing and two-photon absorption in a nonlinear medium. The state is known as pair coherent state and defined as the eigenstate of two operators [1, 2]

$$\hat{a}_1\hat{a}_2|\mu,q\rangle=\mu|\mu,q\rangle,\qquad(\hat{n}_1-\hat{n}_2)|\mu,q\rangle=q|\mu,q\rangle,\tag{1.1}$$

M. Sebawe Abdalla (✉)
Mathematics Department, College of Science, King Saud University, P.O. Box 2455, Riyadh 11451, Saudi Arabia
e-mail: m.sebaweh@physics.org

A.S.-F. Obada
Mathematics Department, Faculty of Science, Al-Azhar University, Nasr City, 11884 Cairo, Egypt

M. Darwish
Department of Physics, Makkah University College, Umm Al-Qura University, Makkah, Saudi Arabia

where $\hat{a}_1$ and $\hat{a}_2$ are the annihilation operators of the field modes, $\hat{n}_i = \hat{a}_i^\dagger \hat{a}_i, i = 1, 2$, is the field photon number while q is an integer while μ a complex number. Another scheme to generate such state is to generate a vibrational pair of coherent states via the motion of a trapped ion in a two-dimensional trap [3]. In the meantime there is another kind of the nonclassical state of electromagnetic field which can be generated using a trapped-ion system, see for example [4]. The state is called a finite dimensional pair-coherent states (FPCS) and is given by

$$|\xi, q\rangle = N_q \sum_{n=0}^{q} \xi^n \sqrt{\frac{(q-n)!}{q!n!}} |q-n, n\rangle, \tag{1.2}$$

where ξ is a complex variable (the state parameter) and q is a positive integer (the difference between the sum of the photon numbers) while N_q is the normalization constant given by

$$N_q = \left[\sum_{n=0}^{q} |\xi|^{2n} \frac{(q-n)!}{q!n!}\right]^{-\frac{1}{2}} = [{}_1F_0(-q, -|\xi|^2)]^{-\frac{1}{2}} \tag{1.3}$$

which ${}_1F_0(.)$ being a generalized hypergeometric function. It would be pointed out that the derivation of the state is analogous to the usual pair coherent state. This can be seen from the state definition which is the eigenstate of the pair operators $(\hat{a}_1^\dagger \hat{a}_2 + \frac{(\hat{a}_1 \hat{a}_2^\dagger \xi)^q}{(q!)^2} \xi)$ for the two modes and the sum of the photon number operators for the two modes, namely

$$\left(\hat{a}_1^\dagger \hat{a}_2 + \frac{(\hat{a}_1 \hat{a}_2^\dagger \xi)^q}{(q!)^2} \xi\right) |\xi, q\rangle = \xi |\xi, q\rangle,$$
$$(\hat{a}_1^\dagger \hat{a}_1 + \hat{a}_2^\dagger \hat{a}_2) |\xi, q\rangle = q |\xi, q\rangle. \tag{1.4}$$

In fact this state has been used by two of the authors in their study of the entropy and variance squeezing for two coupled oscillators in interaction with a two-level atom [5]. Among many of the nonclassical states of light introduced in the literature one can see the present FPCS has the expansion in the number (Fock) states $|n_1, n_2\rangle$ of the two modes as fundamental basis. This is due to the concept of the photon in the quantum theory of the radiation field which is essentially based upon the number state. Therefore, the possibility of generating appropriate squeezed states corresponding to such (number) state is worth considering for at least its fundamental importance [6–8]. This means that the input field in a squeezing device may be generally considered as a superposition of number states rather than a vacuum state or a coherent state, where the last two states are limiting cases of the squeezed state. In fact this has encouraged many authors to examine the effect of squeezing on different kinds of states such as number state [9–11], thermal field state [12, 13], generalized binomial state [14] and nonlinear binomial state [15]. In the present communication we discuss the effect of the two-mode squeezing operator $\hat{S}(r)$ (correlated squeezing operator) on finite dimensional pair-coherent state FPCS. The correlated squeezing operator is essentially generated from the evolution operator of the interaction part of the parametric amplifier model and is given by [16]

$$\hat{S}(r) = \exp[r(\hat{a}_1^\dagger \hat{a}_2^\dagger - \hat{a}_1 \hat{a}_2)], \quad r > 0, \tag{1.5}$$

where r is the squeezing parameter and $\hat{a}_i^\dagger (\hat{a}_i), i = 1, 2$, are the creation and annihilation operators satisfying the commutation relation $[\hat{a}_i, \hat{a}_j^\dagger] = \delta_{ij} = 1$ if $i = j$ and *zero* otherwise.

The squeezed finite-dimensional pair-coherent state (SFPCS) is obtained when one acts by the squeezing operator $\hat{S}(r)$ on the state given by the (1.2). Thus

$$|r,\xi,q\rangle = \hat{S}(r)|\xi,q\rangle. \tag{1.6}$$

Such a state can be generated by applying the Hamiltonian representing the parametric down-conversion of a single photon from a strong field (that can be described classically) onto only two nondegenerate photon on the input state (1.4).

In what follows we discuss some statistical properties of this state and therefore we devote Sect. 2 to consider the normal squeezing and the Glauber second-order correlation function. We also discuss the variance of the photon number sum and difference in addition to the linear correlation function. In Sect. 3 we consider the quasiprobability distribution functions, more precisely W-Wigner and Q-function. This is followed by Sect. 4 which is devoted to discuss the probability and phase distribution. Finally we give our conclusion in Sect. 5.

2 Nonclassical Properties

To discuss the nonclassical properties of the squeezed finite-dimensional pair-coherent state SFPCS we consider two different phenomena. The first is the squeezing phenomenon which can be quantified via the quadrature variances for the normal squeezing case while the second phenomenon is Poissonian and sub-Poissonian behavior which can be measured using the Glauber second-order correlation function. As is well known, the squeezing means reduction in the noise of an optical signal below the vacuum limit, in addition to the possibility of potential applications in optical detection in communications networks of gravitational waves [17–22]. Therefore to discuss the squeezing phenomenon we have to calculate the Hermitian quadrature variances, $\hat{X}$ and $\hat{Y}$, which are related to the conjugate electric and magnetic field $\hat{E}$ and $\hat{H}$. These quadrature operators satisfy the commutation relation $[\hat{X},\hat{Y}] = i\hat{C}$, where $\hat{C}$ may be an operator or C-number depending upon which kind of squeezing we want to discuss. In order to facilitate our discussion we consider the superposition-mode quadrature phases given by [16]

$$\begin{aligned}\hat{X} &= \frac{1}{2}[(\hat{a}_1+\hat{a}_1^\dagger) - \{\hat{a}_2\exp(i\phi)+\hat{a}_2^\dagger\exp(-i\phi)\}],\\ \hat{Y} &= \frac{i}{2}[(\hat{a}_1^\dagger-\hat{a}_1) - \{\hat{a}_2^\dagger\exp(-i\phi)-\hat{a}_2\exp(i\phi)\}],\end{aligned} \tag{2.1}$$

where ϕ is arbitrary phase. To do so we have calculated the expectation values of the photon numbers which give us

$$\begin{aligned}\langle\hat{a}_1^\dagger\hat{a}_1\rangle &= q+(1+q)\sinh^2 r - N_q^2\sum_{n=1}^{q}|\xi|^{2n}\frac{(q-n)!}{q!(n-1)!},\\ \langle\hat{a}_2^\dagger\hat{a}_2\rangle &= (1+q)\sinh^2 r + N_q^2\sum_{n=1}^{q}|\xi|^{2n}\frac{(q-n)!}{q!(n-1)!}.\end{aligned} \tag{2.2}$$

In the meantime we find $\langle\hat{a}_1\rangle = \langle\hat{a}_2\rangle = 0$. Therefore the quadrature variances for the SFPCS are given by

$$\begin{aligned}\langle(\Delta\hat{X})^2\rangle &= \frac{1}{2}(q+1)(\cosh 2r - \cos\phi\sinh 2r),\\ \langle(\Delta\hat{Y})^2\rangle &= \frac{1}{2}(q+1)(\cosh 2r + \cos\phi\sinh 2r).\end{aligned} \tag{2.3}$$

As one can see the fluctuations in $\hat{X}$ may be squeezed below the vacuum level of $\frac{1}{2}$ for $\phi \in [0, \pi/2)$, while the fluctuations in $\hat{Y}$ are enhanced by the correlations. Further, if the phase ϕ is changed to the range $\phi \in (\pi/2, \pi]$, the squeezing occurs in the second quadrature. The effect of the parameter q in this case is just to increase or decrease the amount of the squeezing while the effect of the parameter ξ is absent.

However, for the case in which $\phi = \pi/2$, the phenomenon of squeezing disappeared from the quadrature variances where,

$$\langle (\Delta \hat{X})^2 \rangle = \langle (\Delta \hat{Y})^2 \rangle = \frac{1}{2}(q+1)\cosh 2r.$$

Thus we may conclude that, the phenomenon of squeezing occurs for $\phi \in [0, \pi]$ except at $\phi = \pi/2$ where both quadratures are equal.

As a second example of the nonclassical effect we introduce in this paper the correlation function

$$g_i^{(2)}(\xi) = 1 + \frac{\langle (\Delta \hat{n}_i)^2 \rangle - \langle \hat{n}_i \rangle}{\langle \hat{n}_i \rangle^2}, \quad i = 1, 2. \tag{2.4}$$

To discuss the Glauber second-order correlation function we have to calculate the second moment of the photon numbers. For the first mode we find

$$\langle (\hat{a}_1^\dagger \hat{a}_1)^2 \rangle = N_q^2 \sum_{n=0}^{q} |\xi|^{2n} \frac{(q-n)!}{q!n!} \Bigg[(q-n)^2 \cosh^4 r + (n+1)^2 \sinh^4 r + \left\{ \left(n + \frac{1}{2} \right)(q-n) + \frac{1}{4}(q+1) \right\} \sinh^2 2r \Bigg] \tag{2.5}$$

and for the second mode we have

$$\langle (\hat{a}_2^\dagger \hat{a}_2)^2 \rangle = N_q^2 \sum_{n=0}^{q} |\xi|^{2n} \frac{(q-n)!}{q!n!} \Bigg[n^2 \cosh^4 r + (q-n+1)^2 \sinh^4 r + \left\{ n \left(q - n + \frac{1}{2} \right) + \frac{1}{4}(q+1) \right\} \sinh^2 2r \Bigg]. \tag{2.6}$$

In Fig. 1 we have displayed the behavior of the correlation function for each mode against the parameter ξ for different values of r and q parameters. For example in Fig. 1a we examine the behavior of the correlation function for a fixed value of the parameter $q = 5$ and different values of the squeeze parameter r. In this case we observe that the function shows sub-Poissonian behavior for a small value of ξ. However, it changes its trend to show super-Poissonian behavior and to reach its maximum within short range of ξ. This behavior can be seen for different values of the squeeze parameter r. However, it is more pronounced for a small value of r especially at $r = 0.1$, where thermal distribution can be reported. This phenomenon cannot be seen for the other two values, $r = 0.2$ and $r = 0.5$. In these two cases we can realize that the correlation function reduces its maximum without showing sub-Poissonian or even Poissonian distribution. On the other hand we have plotted the function for a fixed value of the squeeze parameter, $r = 0.5$, but for different values of the q-parameter. In this case we can observe that the function starts with sub-Poissonian behavior and after a small range of ξ it shows super-Poissonian behavior. In fact the function shows sub-Poissonian behavior with a minimum value for $q = 5$, while it exhibits super-Poissonian

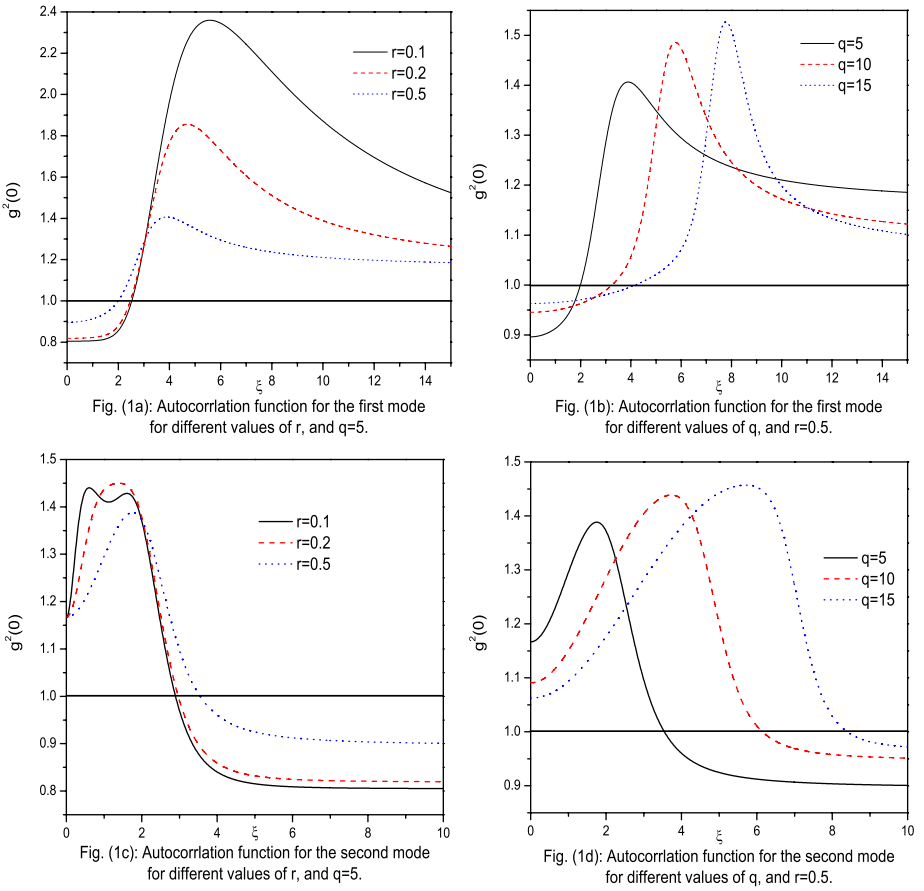

Fig. 1 The autocorrelation function $g^{(2)}(0)$ for different values of the involved parameters as indicated: (**a**) and (**b**) for the first mode and (**c**) and (**d**) for the second mode

behavior with a maximum value for $q = 15$, see Fig. 1b. This means that an increase in the value of the q-parameter leads to an increase in the range of the parameter ξ, where sub-Poissonian behavior occurred, besides an increase in the height of the peak and a shift to higher ξ. It is also noted that the general behavior of the function in this case is nearly similar to that of the previous case, however, for different values of the parameters. The situation is greatly changed when we consider the correlation function for the second mode. In this case and contrary to the first mode the function starts with super-Poissonian behavior with an increase in its peak value. It is easy to realize that the function is then reduced in its value quite drastically showing sub-Poissonian, which is pronounced for a small value of $r = 0.1$. It is also noted that for all values of the squeeze parameter r the correlation function does not return to show super-Poissonian behavior whatever the range of the parameter ξ, see Fig. 1c. Also we have examined the correlation function against ξ for a fixed value of the squeeze parameter, namely $r = 0.5$. In this case we observe that for different ranges of ξ the function exhibits super-Poissonian behavior. However, the maximum value of the function depends upon the value of the q parameter considered, see Fig. 1d. In the meantime we can see sub-Poissonic behavior starts to appear for the case in which $q = 5$, followed by the

other two cases $q = 10$ and 15, respectively. Finally we report that the correlation function in this case reaches its maximum for $q = 15$ and its minimum for $q = 5$. This means that an increase in the photon number leads to an increase in the correlation function value and hence the classical effect would be pronounced.

Now we extend our discussion to include the intensities in the two modes. This can be achieved if one obtains the expression of the variance of the photon number difference and sum. Using the above given equations of the expectation values we have

$$\begin{aligned}\Delta(\hat{a}_1^\dagger \hat{a}_1 - \hat{a}_2^\dagger \hat{a}_2)^2 &= 4\left[N_q^2 \sum_{n=0}^{q} |\xi|^{2n} \frac{(q-n)!}{q!n!} n^2 - \left(N_q^2 \sum_{n=0}^{q} |\zeta|^{2n} \frac{(q-n)!}{q!n!} n\right)^2\right], \\ \Delta(\hat{a}_1^\dagger \hat{a}_1 + \hat{a}_2^\dagger \hat{a}_2)^2 &= N_q^2 \sum_{n=0}^{q} |\xi|^{2n} \frac{(q-n)!}{q!n!} [2n(q-n) + (q+1)] \sinh^2 2r.\end{aligned} \tag{2.7}$$

It is easy for one to compare between the present case and the case of the usual squeezed vacuum-state case. In fact there is an essential difference between the two cases. This can be seen when we measure the photon-number difference. For the squeezed vacuum-state the *zero* variance is a result of the correlation between the modes. However, for the squeezed finite pair coherent state the result is equal to four times the expectation value of the mean photon number for the first mode. In Fig. 2a we have plotted the photon-number difference against the parameter ξ for different values of q ($q = 5, 10, 15$). As one can see, the function shows Gaussian behavior with an increase in its peak value as q increases. In the meantime the function shifts its position in the direction of increasing ξ. This behavior is valid whatever the value of the squeeze parameter r. On the other hand for the photon-number sum the situation is also different where the non zero value of this quantity (which is the signature of the intensity of photon-number correlations between the modes) is sensitive to any variation in both q and r parameters. This can be seen in Figs. 2b, 2c in which we have plotted the photon number sum against the parameter ξ for two different cases. In the first case we have considered the parameter $q = 5$ but with different values of the parameter r. For a small value of the squeeze parameter, $r = 0.1$, the variance is slightly increased in its value and then it returns to decrease it for a large range of ξ. However, when we consider $r = 0.2$, the variance increased its value nearly three times for the same interval of ξ, then it returns again to show a behavior similar to that of the previous case. When we take the squeeze parameter $r = 0.4$, the value of the variance increased rapidly by nearly five times the case in which $r = 0.2$. In the mean time there is no change in the general behavior of the function, see Fig. 2b. In the second case and for fixed value of the squeeze parameter, $r = 0.4$, we can see an increase in the maximum value of the function as the q parameter increases. Also we note a shift to the right towards higher values of ξ. However, the function shows asymptotic behavior for large values of ξ, see Fig. 2c.

Now we turn our attention to consider the linear correlation function defined by

$$\mathcal{L}(n_1, n_2) = \frac{\langle n_1 n_2 \rangle - \langle n_1 \rangle \langle n_2 \rangle}{\sqrt{\langle (\Delta n_1)^2 \rangle \langle (\Delta n_2)^2 \rangle}}, \tag{2.8}$$

where the quadrature variances $\langle (\Delta n_i)^2 \rangle, i = 1, 2$, can be obtained from (2.2), (2.5) and (2.6). In Fig. 2d we have plotted the linear correlation function against the parameter ξ for different values of q ($q = 1, 2, 3$) and a fixed value of the squeeze parameter, $r = 1$. In this case the functions have different values, each one depends upon the value of the q parameter and follows the relation $\mathcal{L}(n_1, n_2) = q^2$. This can be realized from Fig. 2d. This indicates that

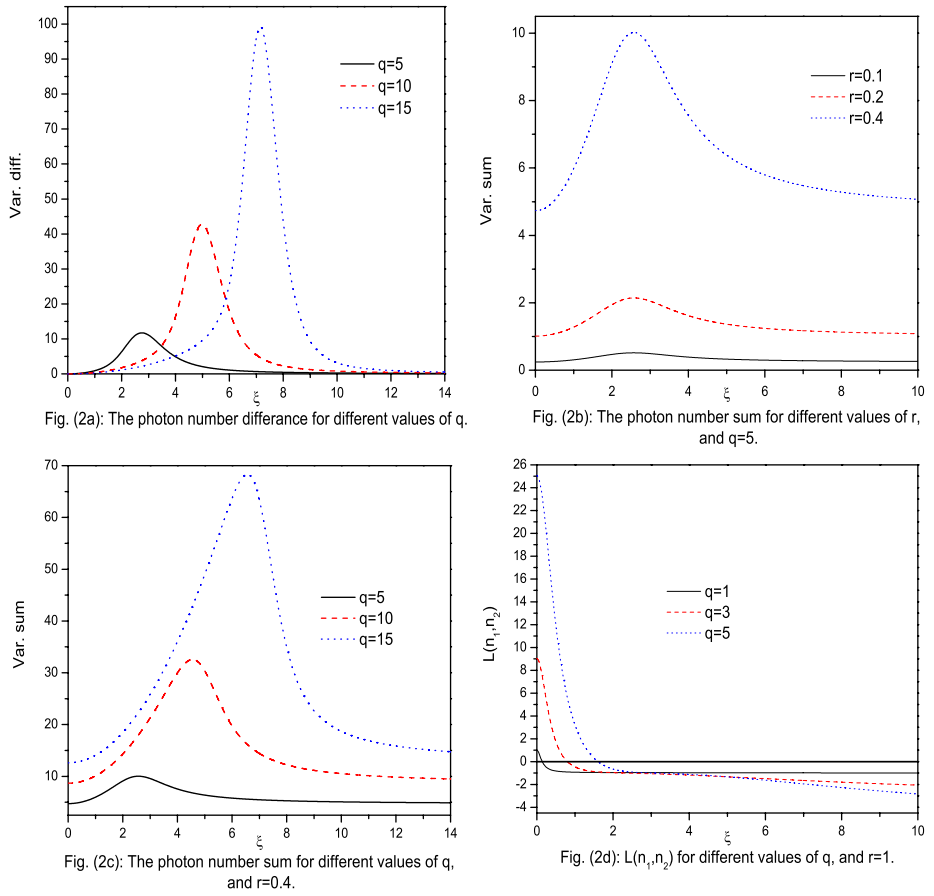

Fig. (2a): The photon number differance for different values of q.

Fig. (2b): The photon number sum for different values of r, and q=5.

Fig. (2c): The photon number sum for different values of q, and r=0.4.

Fig. (2d): $L(n_1,n_2)$ for different values of q, and r=1.

Fig. 2 The variance of the photon number difference and sum as well as the linear correlation for different values of the involved parameters as indicated: (**a**) The photon number difference for different value of q and fixed value of r. (**b**) The photon number sum for fixed value of q and different values of r. (**c**) The photon number sum for fixed value of r and different values of q. (**d**) The linear correlation for fixed value of r and different values of q

for a large value of q the two modes are strongly correlated. However, this high correlation only occurs for a small value of ξ. Increasing the value of ξ leads to anticorrelation which is firstly observed for $q = 1$, where the function in this case shows almost constant value. This is not the case for $q = 3$ and 5 where the function continue to decrease its value as ξ increases. We have also examined the effect of the squeeze parameter (not displayed here) on the linear correlation function assuming that $r = 0.1, 0.2, 0.3$ and $q = 3$. In this case similar behavior to that of the previous case can be reported. However, only one difference can be mentioned in this case. After the interval of strong correlation the function starts to show anticorrelation which gets more pronounced as the value of both r and ξ increases. Therefore, it is concluded that the correlation between the modes can be controlled by a judicial choice of the parameters of the state especially the parameter ξ in addition to r and q.

3 Quasiprobability Distribution

In this section we consider the quasiprobability distribution functions. These well-known functions are P-representation, W-Wigner and Q-function and are regarded as important tools to provide insight into the nonclassical features of the radiation fields. In fact they have advantages connected with their use. As a part of the advantages of the Wigner function may become negative for some quantum states, it has the considerable advantage for squeezed states that its contour maps the variances in the field quadratures. The Q-function is a positive-definite quasiprobability distribution, but its simple relation to antinormal operator products makes it difficult to interpret in terms of conventional photon counting or squeezing measurements. They are defined by taking the Fourier transforms of their respective characteristic functions:

$$I(\alpha,\beta,s)=\frac{1}{\pi^4}\int_{-\infty}^{\infty}d^2\zeta d^2\eta\exp(\alpha\eta^*-\alpha^*\eta)\exp(\beta\zeta^*-\beta^*\zeta)C(\zeta,\eta,s), \tag{3.1}$$

where $C(\zeta,\eta,s)$ is the s-parameterized characteristic function with the parameter, $s=1,0,-1$ corresponding to P-representation, W-Wigner and Q-function, respectively. The s-parameterized characteristic function is evaluated through the relation

$$C(\zeta,\eta,s)=\mathrm{Tr}\Bigg\{\hat{\rho}\exp(\hat{a}_1^{\dagger}\eta-\hat{a}_1\eta^*)\exp(\hat{a}_2^{\dagger}\zeta-\hat{a}_2\zeta^*).\times\exp\bigg[\frac{s}{2}(|\eta|^2+|\zeta|^2)\bigg]\Bigg\}, \tag{3.2}$$

whereas $\hat{\rho}$ is the density matrix which is given for the squeezed finite dimensional pair-coherent state by

$$\hat{\rho}=|r,\xi,q\rangle\langle r,\xi,q|. \tag{3.3}$$

In what follows we consider the W-Wigner and the Q-function by evaluating the integral in (3.1) for $s=0$ and $s=-1$, respectively. This can be achieved if one calculates the characteristic function $C(\zeta,\eta,s)$. When $s\neq 0$, we have the expression

$$\begin{aligned}C(\zeta,\eta,s)=\exp\bigg[-\frac{1}{2}(|\zeta|^2+|\eta|^2)(\cosh 2r-s)+\frac{1}{2}(\zeta\eta+\zeta^*\eta^*)\sinh 2r\bigg]\\ \times N_q^2\Bigg\{\sum_{n=0}^{q}\frac{(q-n)!}{q!n!}|\xi|^{2n}L_n(|\bar{\eta}|^2)L_{(q-n)}(|\bar{\zeta}|^2)\\ +\sum_{\substack{n,m=0\\ n>m}}^{q}\bigg[\frac{(q-n)!}{q!m!}\xi^n\xi^{*m}\bigg(\frac{\bar{\eta}}{\bar{\zeta}}\bigg)^{m-n}\bigg]L_n^{(m-n)}(|\bar{\eta}|^2)L_{(q-n)}^{(n-m)}(|\bar{\zeta}|^2)\Bigg\},\end{aligned} \tag{3.4}$$

where $L_n^s(x)$ are the well-known Laguerre polynomials given by

$$L_n^{(\gamma)}(x)=\sum_{k=0}^{n}\frac{(-1)^k x^k(n+\gamma)!}{k!(n-k)!\Gamma(k+\gamma+1)},\quad \gamma=0,1,2,\ldots, \tag{3.5}$$

and

$$\bar{\zeta}=\zeta\cosh r-\eta^*\sinh r,\quad \bar{\eta}=\eta\cosh r-\zeta^*\sinh r. \tag{3.6}$$

It should be noted that the diagonal part of the characteristic function $C(\zeta,\eta,s)$ is not normalized quantity. Having obtained the characteristic function we are therefore in a position to find W-Wigner and Q-functions. This is done in the following subsections.

3.1 Wigner Function

To obtain the Wigner function we have to insert (3.4) into (3.1) and perform the integral. In this case we have for $s=0$ the Wigner function in the form

$$\begin{aligned} W(\alpha,\beta,r) = {} & \frac{4\cos\pi q}{\pi^2} N_q^2 \exp[-2(|\bar{\alpha}|^2+|\bar{\beta}|^2)] \\ & \times \Bigg\{ \sum_{n=0}^{q} \frac{(q-n)!}{q!n!} |\xi|^{2n} L_n(4|\bar{\alpha}|^2) L_{(q-n)}(4|\bar{\beta}|^2) \\ & + 2 \sum_{\substack{n,m=0 \\ n>m}}^{q} \left[\frac{(q-n)!}{q!m!} \xi^n \xi^{*m} \left| \frac{\bar{\beta}}{\bar{\alpha}} \right|^{(n-m)} \right] L_n^{(m-n)}(4|\bar{\alpha}|^2) \\ & \times L_{(q-n)}^{(n-m)}(4|\bar{\beta}|^2) \cos[(\bar{\theta}+\bar{\phi})(n-m)] \Bigg\}, \end{aligned} \tag{3.7}$$

where $\bar{\alpha}$ and $\bar{\beta}$ are the eigenvalues of the squeezed coherent states given by

$$\bar{\alpha} = \alpha\cosh r - \beta^* \sinh r, \quad \bar{\beta} = \beta\cosh r - \alpha^* \sinh r, \tag{3.8}$$

while $\bar{\theta}$ and $\bar{\phi}$ are the phase angles of $\bar{\alpha}$ and $\bar{\beta}$, respectively.

From (3.7) we can deduce that the diagonal form of the Wigner function takes the expression

$$\begin{aligned} W(\alpha,\beta,r) = {} & \frac{4\cos\pi q}{\pi^2} N_q^2 \exp[-2(|\bar{\alpha}|^2+|\bar{\beta}|^2)] \\ & \times \sum_{n=0}^{q} \frac{(q-n)!}{q!n!} |\xi|^{2n} L_n(4|\bar{\alpha}|^2) L_{(q-n)}(4|\bar{\beta}|^2). \end{aligned} \tag{3.9}$$

In Fig. 3 we have plotted the diagonal case of the Wigner function against $x=\operatorname{Re}\alpha$ and $y=\operatorname{Im}\alpha$ for different values of β and ξ besides q and r parameters. In general the function shows behavior in which the negative values appear, reflecting nonclassical effects. However, its shape varies as we change the values of the parameter. As a result of the appearance of the factor $\cos\pi q$ in (3.9) it is expected that, the function would show a negative peak at the origin for odd q and show a positive peak for even q. For example, when we consider the case in which $r=\beta=\xi=0.1$ and $q=5$, the function shows oscillations around the center with a sharp peak downwards at the middle of the base showing negative value, see Fig. 3a. However, when we increase the value of the q parameter ($q=10$) without changing the other parameter values, different behavior to the previous case can be observed. The main difference between the two cases is that; we observe a wide base with an increase in the oscillations around the center, while the sharp peak changes its direction to be upwards at the middle of the base showing positive-valued peak, see Fig. 3b. This behavior is expected from the structure of the function given by (3.9), where the existence of the sinusoidal function is apparent as mentioned above. Thus we can conclude that increasing the value of the

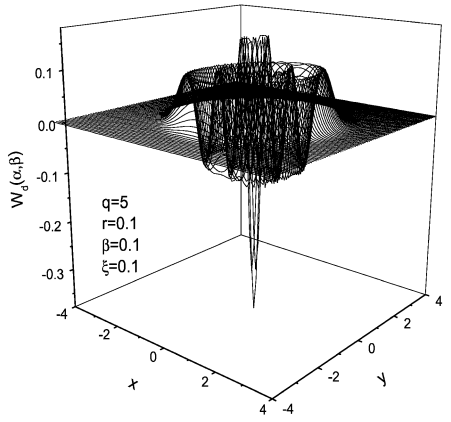

Fig. 3a: Wigner Function in diagonal case.

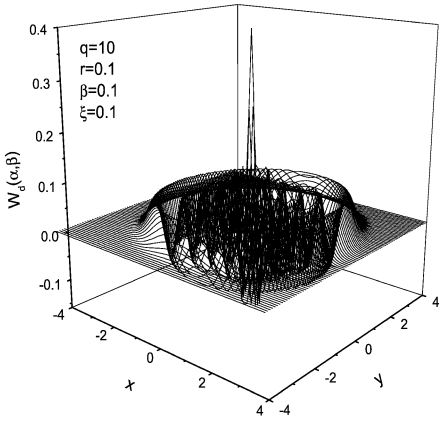

Fig. 3b: Wigner Function in diagonal case.

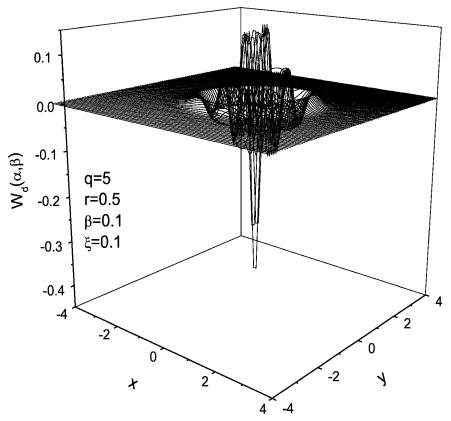

Fig. 3c: Wigner Function in diagonal case.

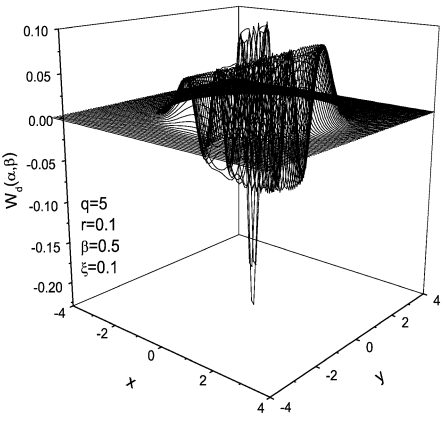

Fig. 3d: Wigner Function in diagonal case.

Fig. 3 The Wigner function in the diagonal case for different values of the involved parameters as indicated

parameter q leads to a reduction in the nonclassical by negative values. On the other hand, when we take the value of the squeeze parameter $r = 0.5$, the nonclassical effect gets more pronounced where the function shows reduction in its oscillations besides a shrinking in its base toward the center, see Fig. 3c. To examine the behavior of the function at different values of β we have increased its value from 0.1 to 0.5. In this case we observe the function losing the symmetry around the center. Also there is a shrinking of the peak from -0.4 to -0.2, see Fig. 3d. This means that an increase in the value of the coherent variable β means departing from the center, which leads consequently to decrease in the nonclassical effect. This may be attributed to the exponential factor $\exp(-2|\beta|^2)$ appearing in the expression for the Wigner function. To examine the effect of the ξ parameter on the Wigner function we have considered the case in which $\xi = 0.5$. In this case we have observed that there is no substantial change in the behavior of the function and the shape of the function is similar to that of Fig. 3a with the parameters as previously fixed.

We now turn our attention to examine the behavior of the Wigner function when the off-diagonal terms are taken into account. For this reason we have plotted the function against $x = \mathrm{Re}\,\alpha$ and $y = \mathrm{Im}\,\alpha$ for different values of β, as well as for the parameters ξ, q and r,

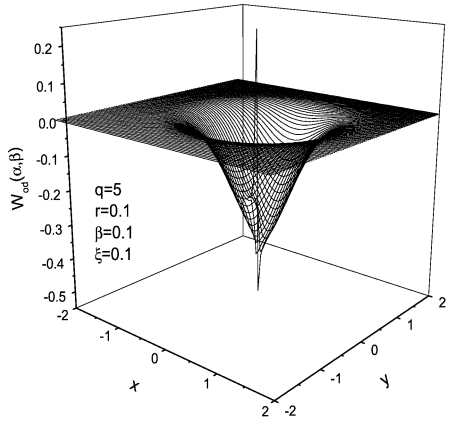

Fig. 4a: Wigner Function in off diagonal case.

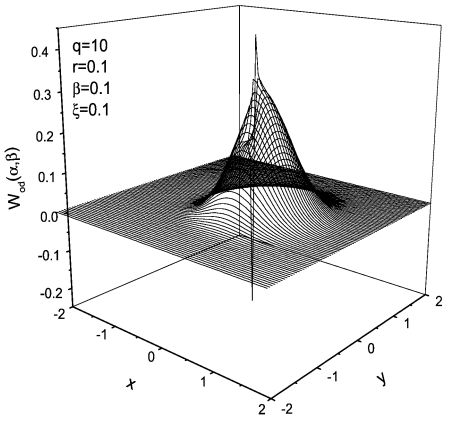

Fig. 4b: Wigner Function in off diagonal case.

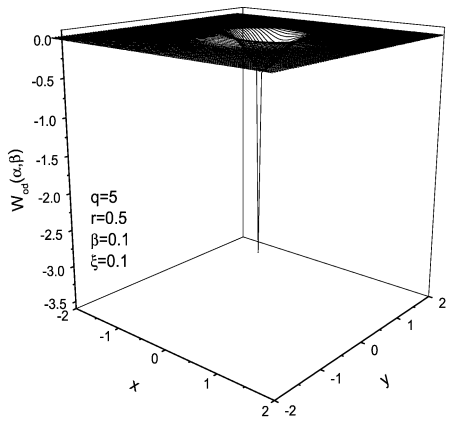

Fig. 4c: Wigner Function in off diagonal case.

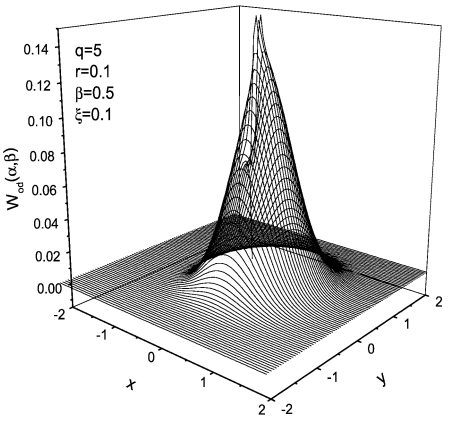

Fig. 4d: Wigner Function in off diagonal case.

Fig. 4 The Wigner function in the off-diagonal case for different values of the involved parameters as indicated

see Fig. 4. In Fig. 4a we display the function for the case in which $r = \beta = \xi = 0.1$ and $q = 5$ where one can see a peak goes off from a flat base with a hole at the center. The peak gets sharper as its value decreases where it shows negative value with minimum at -0.5. This in fact reflects the nonclassical behavior of the state in presence of the squeeze parameter. Increasing the value of the parameter q leads to a reduction in the nonclassical behavior, where the peak changes its direction upwards showing positive values for even q. Although the effect of the squeezing gets weak, we can see a very thin negative peak at the center of the base, see Fig. 4b. A dramatic change can be seen when we increase the value of the squeeze parameter, $r = 0.5$. In this case the base shrinks around the center and the negative value of the peak gets pronounced, see Fig. 4c. The opposite behavior for Fig. 4c can be seen in Fig. 4d for the case in which $\beta = 0.5$, where the effect of the squeezing is slightly apparent. This means that the effect of the coherent variable β is stronger than the effect of the squeeze parameter and consequently the nonclassical behavior is almost obliterated.

3.2 The Q-function

A second task of the present section is to consider the Q-function. In what follows we restrict ourself with the diagonal terms and therefore we have to evaluate the integral

$$\begin{aligned} Q(\alpha,\beta,r) &= \frac{1}{\pi^4}\sum_{n=0}^{q}\frac{(q-n)!}{q!n!}|\xi|^{2n} \\ &\times \int_{-\infty}^{\infty} d^2\bar{\zeta}\,d^2\bar{\eta}\exp[(\bar{\zeta}^*\bar{\beta}-\bar{\zeta}\bar{\beta}^*)+(\bar{\eta}^*\bar{\alpha}-\bar{\eta}\bar{\alpha}^*)] \\ &\times \exp\left[-\left((|\bar{\eta}|^2+|\bar{\zeta}|^2)\cosh^2 r+\frac{1}{2}(\bar{\eta}\bar{\zeta}+\bar{\eta}^*\bar{\zeta}^*)\sinh 2r\right)\right] \\ &\times L_n(|\bar{\eta}|^2)L_{(q-n)}(|\bar{\zeta}|^2). \end{aligned} \tag{3.10}$$

After a lengthy but straightforward calculation we have the expression

$$\begin{aligned} Q(\alpha,\beta,r) &= \frac{\operatorname{sech}^2 r}{\pi^2}\exp[-(|\bar{\alpha}|^2+|\bar{\beta}|^2)+(\bar{\alpha}\bar{\beta}+\bar{\alpha}^*\bar{\beta}^*)\tanh r] \\ &\times N_q^2\sum_{n=0}^{q}\frac{(q-n)!|\xi|^{2n}}{2^{2n}q!n!}\sum_{k=0}^{n}\sum_{s=0}^{m}\frac{(-)^{(k-s)}(2k)!(2m-2s)!}{k!s!(n-k)!(m-s)!} \\ &\times [(\bar{\beta}+\bar{\beta}^*)\tanh r-(\bar{\alpha}+\bar{\alpha}^*)]^{2(n-m)}(2\tanh r)^{2(k-s)} \\ &\times \left(\frac{1}{2}\frac{[(\bar{\alpha}+\bar{\alpha}^*)\coth r-(\bar{\beta}+\bar{\beta}^*)]}{[(\bar{\beta}-\bar{\beta}^*)+(\bar{\alpha}-\bar{\alpha}^*)\tanh r]}\right)^{2(s-k)} \\ &\times L_{2s}^{2(k-s)}(u)L_{(2m-2s)}^{(2n-2k)-(2m-2s)}(v), \quad m=(q-n), \end{aligned} \tag{3.11}$$

where

$$\begin{aligned} u(\alpha,\beta) &= \frac{1}{2}[(\bar{\alpha}^*-\bar{\alpha})\coth r+(\bar{\beta}^*-\bar{\beta})][(\bar{\alpha}-\bar{\alpha}^*)\tanh r+(\bar{\beta}-\bar{\beta}^*)], \\ v(\alpha,\beta) &= \frac{1}{2}[(\bar{\alpha}+\bar{\alpha}^*)\tanh r-(\bar{\beta}+\bar{\beta}^*)][(\bar{\alpha}+\bar{\alpha}^*)\coth r-(\bar{\beta}+\bar{\beta}^*)]. \end{aligned} \tag{3.12}$$

As a special case, if we consider the squeeze parameter $r=0$, the Q-function reduces to the form

$$Q(\alpha,\beta,r)=\frac{N_q^2}{\pi^2}\exp[-(|\alpha|^2+|\beta|^2)]\sum_{n=0}^{q}\frac{|\xi|^{2n}}{q!(n!)^2}|\alpha|^{2(q-n)}|\beta|^{2n}. \tag{3.13}$$

It should be noted that the Q-function can also be obtained from the equation

$$Q(\alpha,\beta,r)=\frac{1}{\pi^2}|\langle\alpha,\beta|\xi,q,r\rangle|^2 \tag{3.14}$$

and in this case we have the expression

$$\begin{aligned} Q(\alpha,\beta,r) &= \frac{N_q^2}{\pi^2 q!}\exp[-(|\alpha|^2+|\beta|^2)+(\alpha\beta+\alpha^*\beta^*)\tanh r] \\ &\times(\operatorname{sech} r)^{2(q+1)}|G(\alpha,\beta,r)|^2, \end{aligned} \tag{3.15}$$

where

$$G(\alpha,\beta,r)=\sum_{n=0}^{q}\sum_{l=0}^{\min(n,q-n)}\xi^{n}\frac{(q-n)!\tanh^{n}r\cosh^{2l}r}{l!(q-n-l)!(n-l)!}(\alpha^{*})^{(q-n-l)}(\beta^{*})^{n-l}. \tag{3.16}$$

It is clear from (3.11) that the Q-function has a complicated expression from which we are not able to analyze its shape. To tackle this situation we have to make some numerical computations and plot some figures to display its behavior for different values of the parameters involved. Some details of behavior can be seen if the function is plotted against $\mathrm{Re}\,\alpha$ and $\mathrm{Im}\,\alpha$ for some different values of β and ξ as well as for the parameters q and r. This has been done in Fig. 5 in which we can see in the absence of the squeeze parameter r and for $\beta=\xi=0.1$ and $q=3$ that the function has a doubly folded peak in the center towards the positive side. This means that the Q-function shows Fock-state behavior, see Fig. 5a. To study the effect of the squeezing on the Q-function we set the parameter $r=0.1$. In this case the radius of the base decreases and two opposite sides of the rim are increasing, see Fig. 5b. Increasing the squeezing parameter to $r=0.15$, leads to an increase in the rim sides, see Fig. 5c. When we examine the effect of the q parameter and consider $\beta=\xi=r=0.1$ while $q=5$, we observe that the doubly folded peak greatly decreases its value while its base widens. This indicates that the effect of the q parameter becomes stronger than the effect the squeeze parameter r. Finally we examine the behavior of the function at a fixed value of β that represents the coherent field. In this case and for $\beta=0.5$ we observe a breaking of the symmetry of the function where one side of the base rim increases corresponding to a decrease in the other side. Also we realize that there is a slight reduction in the Q-function height. This can be seen from the appearance of the factor $\exp(-|\beta|^{2})$ in the expression for the Q-function which reduces the height of the function. However, the effect of the squeeze parameter still survives beside the appearance of the asymmetry, see Fig. 5e.

4 The Quadrature and Phase Distribution Functions

In this section we wish to examine the behavior of the quadrature distribution function as well as the phase distribution functions against the parameters involved. To reach our goal we have to employ the Wigner function $W(\alpha,\beta,r)$ given by (3.9), where we restrict our treatment to the diagonal terms. This is achieved in the next subsections.

4.1 The Quadrature Distribution Function

To calculate the quadrature distribution function $P(x,y,r)$ we have to integrate the function $W(\alpha,\beta,r)$ over the imaginary variable for both α and β, such that [15, 23, 24]

$$P(x,y,r)=\int_{-\infty}^{\infty}W(\alpha,\beta,r)d\,\mathrm{Im}\,\alpha d\,\mathrm{Im}\,\beta. \tag{4.1}$$

In this case if we insert (3.9) into (4.1) and after a straightforward calculation,we find that the distribution function $P(x,y,r)$ takes the form

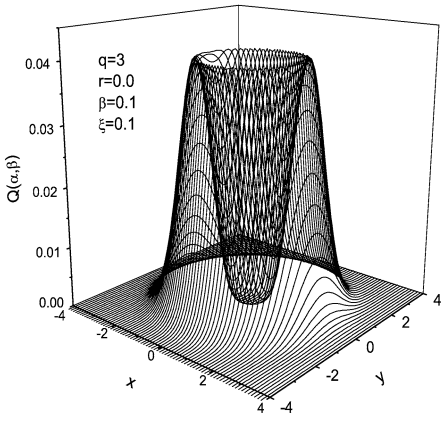

Fig. 5a: Q-Function as a function of α, β.

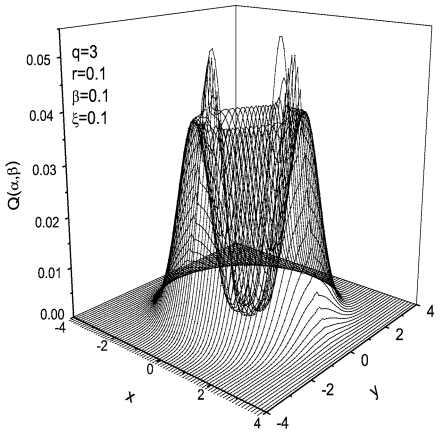

Fig. 5b: Q-Function as a function of α, β.

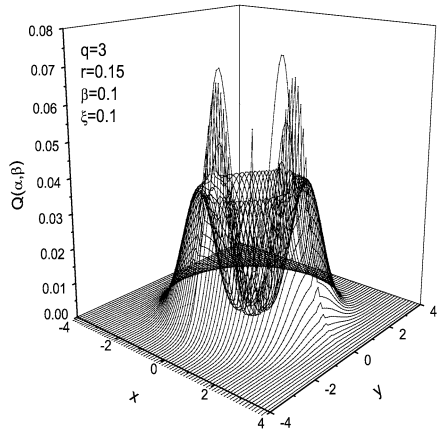

Fig. 5c: Q-Function as a function of α, β.

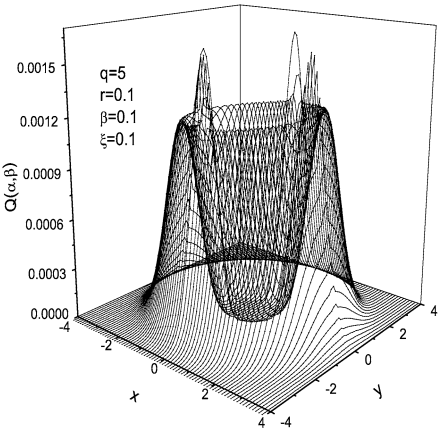

Fig. 5d: Q-Function as a function of α, β.

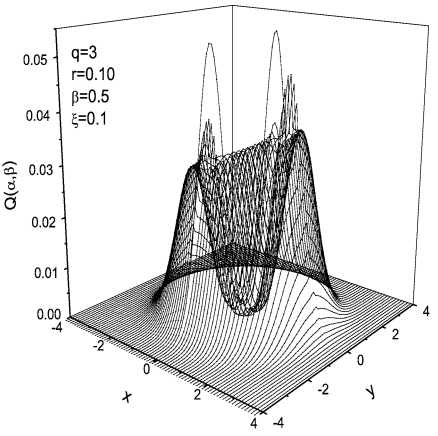

Fig. 5e: Q-Function as a function of α, β.

Fig. 5 The Q-function in the diagonal case for different values of the involved parameters as indicated

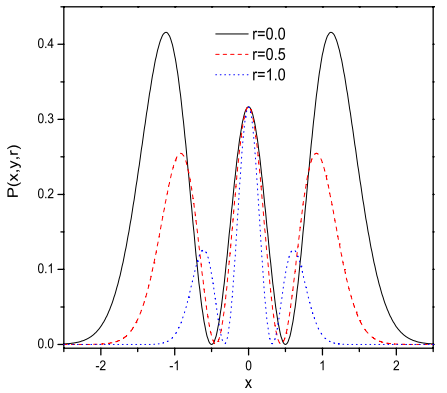

Fig. (6a):The position distribution function at y=0, q=2 and ξ=0.1.

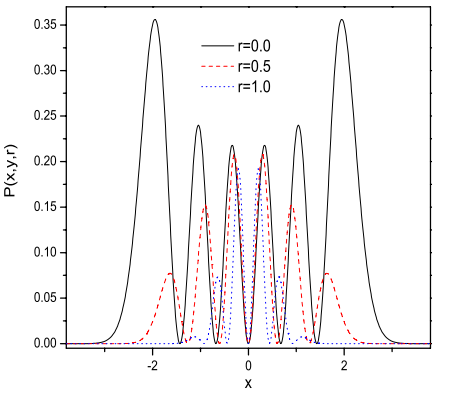

Fig. (6b):The position distribution function at y=0, q=5 and ξ=0.1.

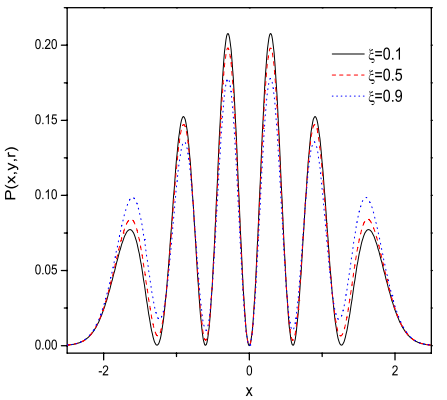

Fig. (6c):The position distribution function at y=0, q=5 and r=0.5.

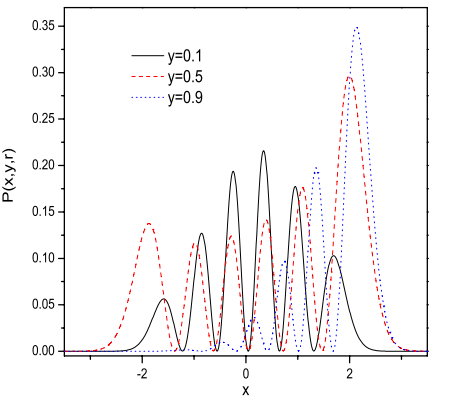

Fig. (6d):The position distribution function at ξ=0.1, q=5 and r=0.5.

Fig. 6 The distribution function $P(x, y, r)$ in the diagonal case for different values of the involved parameters as indicated

$$P(x, y, r) = \frac{2}{\pi} N_q^2 \sum_{n=0}^{q} \frac{2^{-q}|\xi|^{2n}}{q!(n!)^2} H^2_{(q-n)}(\sqrt{2}\bar{x}) H_n^2(\sqrt{2}\bar{y}) \times \exp\{-2[(x^2 + y^2)\cosh 2r - 2xy \sinh 2r]\}, \tag{4.2}$$

where

$$\bar{x} = x \cosh r - y \sinh r, \quad \bar{y} = y \cosh r - x \sinh r. \tag{4.3}$$

In Fig. 6 we have plotted the distribution function $P(x, y, r)$ against x for different values of the parameters involved. For instance we examine the function's behavior for a fixed value of $y = 0$, $q = 2$ and $\xi = 0.1$. In this case and for different values of the squeezing parameter, r, the function has a positive value and shows regular fluctuations with a symmetry around $x = 0$. In the meantime the maximum height of the function is exhibited for the case in which $r = 0$ at the two outer peaks. We also observe that increasing the value of the squeezing parameter results in decreasing the amplitude of the function. This is quite obvious for the cases in which $r = 0, 0.5$ and 1.0, see Fig. 6a. It is also noted that the maximum value

of the function at $r = 0$ occurs at shorter distances than for the other two cases. When we increase the value of the q parameter to $q = 5$, the number of the oscillations increases while their amplitude decreases. However, there is no change for the symmetry around $x = 0$, see Fig. 6b. Here we may point out that the number of the peaks for all the cases is always equal to $q + 1$. Now we turn our attention to consider the effect of the ξ parameter on the distribution function when we set $y = 0, q = 5$ and $r = 0.5$. As one can see from Fig. 6c, the function for $\xi = 0.1$ shows regular fluctuations as well as a symmetry around $x = 0$. Also it is noted that the heights of the peaks increase until $x = 0$ is reached. Then they start to decrease as one moves away. When we increase the value of ξ, for example, $\xi = 0.5$ the maximum value of the peak at the beginning and at the end of the interval gets higher than that for the case in which $\xi = 0.1$. This behavior gets more pronounced for the case in which $\xi = 0.9$. Finally we consider the variation that occurs in the distribution function due to the change in the real part of the coherent parameter β. In this case and for $y = 0.1$ the function starts to increase its value after a certain interval of x with maximum value approximately around $\sim$0.05. This value is less than that for the case in which $y = 0$, see Fig. 6c where the maximum value occurs at $\sim$0.075. This is due to the appearance of $\exp(-2y^2)$ which amounts to lowering the value of the function. However, the function increases its value when we consider $y = 0.5$ and we can not see any increment for the case in which $y = 0.9$ during the same interval of x. In the meantime the function shows that its maximum for $y = 0.9$ is greater than that its maximum for $y = 0.5$, however, having a shift at the positive side of x, see Fig. 6d.

4.2 The Phase Distribution

To calculate the phase distribution we have to integrate the function $\frac{1}{4}W(\alpha, \beta, r)$ over the mean photon numbers for each mode. This means that the integration runs over the radius of the coherent parameters for both fields. However, due to the existence of the term $\cos \pi q$ in the Wigner function we have to expect a negative value as a part of the phase distribution. This in addition to the negative value which usually appears due to the nature of the Wigner function. Therefore to avoid this situation we have to consider the Pegg-Barnett phase-distribution formalism [25–28]. When one uses the Pegg-Barnett scheme for calculating the phase properties for a state of a single mode given by $|\psi\rangle = \sum c_n|n\rangle$, then one has to use the phase state introduced by

$$|\theta_m\rangle = \frac{1}{\sqrt{s+1}} \sum_{n=0}^{s} \exp(in\theta_m)|n\rangle, \qquad \theta_m = \theta_0 + \frac{2\pi m}{s+1}, \quad m = 0, 1, 2 \ldots \tag{4.4}$$

The phase probability can be written in the form

$$P_{PB}(\theta) = \lim_{s\to 0} \frac{s+1}{2\pi} |\langle\theta_m|\psi\rangle|^2 = \frac{1}{2\pi} \left| \sum_{n=0}^{\infty} c_n \exp(in\theta) \right|^2. \tag{4.5}$$

This can be generalized to include more than one mode. Therefore, for the present case we have

$$P_{PB}(\theta, \phi, r) = \frac{N_q^2 (\operatorname{sech} r)^{2(q+1)}}{4\pi^2 (q!)} |\mathcal{J}(\theta, \phi, r)|^2, \tag{4.6}$$

where the function $\mathcal{J}(\theta, \phi, r)$ is given by

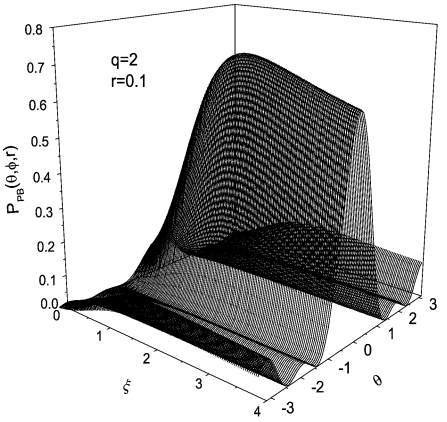

Fig. 7a: The phase distribution function.

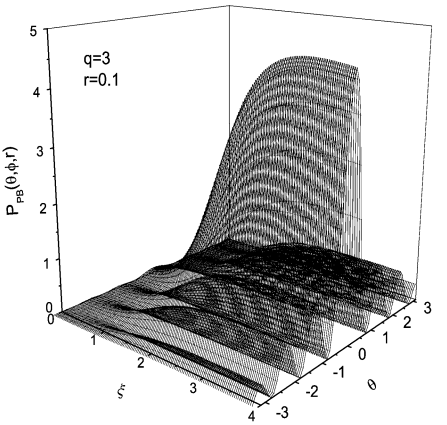

Fig. 7b: The phase distribution function.

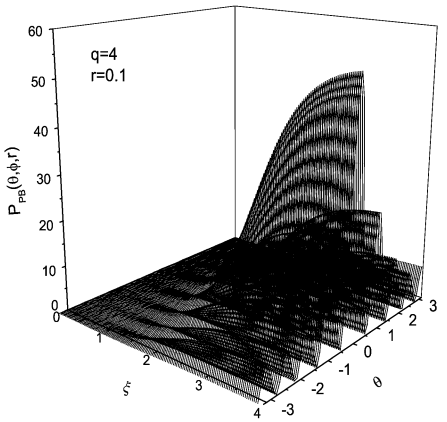

Fig. 7c: The phase distribution function.

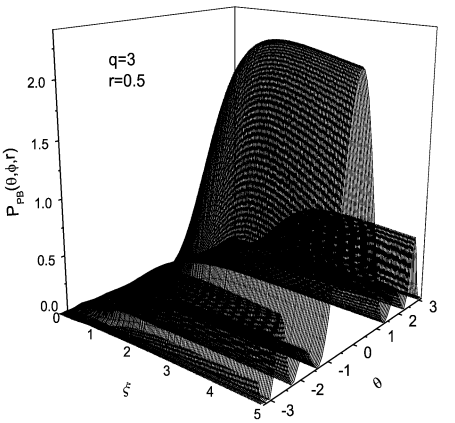

Fig. 7d: The phase distribution function.

Fig. 7 The phase distribution function for different values of the involved parameters as indicated

$$\mathcal{J}(\theta,\phi,r) = \sum_{n=0}^{q} \xi^n \sum_{l=0}^{\min(n,q-n)} \sum_{k=0}^{\infty} C_l^{(q-n)} \frac{\cos \pi k}{k!(n-l)!} \times \sqrt{(q-n-l+k)!(n-l+k)!}(\tanh r)^{k+l} \cosh^{2l} r \times \exp(i(q-n-l+k)\theta + i(n-l+k)\phi). \quad (4.7)$$

From the above equation it is not an easy task to see and analyze the behavior of the function $P_{PB}(\theta,\phi,r)$. Therefore in Fig. 7 we have plotted the function against the parameter ξ and the phase angle θ assuming that the other phase angle $\phi = 0$. Before we go further we observe that for $\xi = 0$ there is no phase information to be reported. However, as ξ increases and there is summation of the Fock states then the phase starts to build up. Moreover, for $\phi = \pi$ the main peak is shifted to the value $\theta = \pi$, which is not displayed here. In Fig. 7a we have considered the case in which $r = 0.1$ and $q = 2$, where the main peak is centered around $\theta = 0$ with a symmetrical behavior. Increasing the value of the parameter q, for example $q = 3$, leads to the appearance of side peaks. The number of these peaks increases

by increasing q in a linear way. This is seen from the comparison between Figs. 7a, 7b and 7c. These peaks start small and gain height as ξ increases until they reach a stationary value. However, they start to lose height by further increasing the value of ξ, see Figs. 7a and 7b. On the other hand the squeezing parameter r shows another trend, for example, when we increase its value such that $r = 0.5$, see Fig. 7d. In this case the number of the peaks is unaltered while their heights are reduced. However, the height of the first side peak is smaller than the second side peak in contrast to the case of Fig. 7b.

5 Conclusion

In the previous sections of the present paper we have examined the effect of the two mode squeeze operator on the finite-pair coherent state. Our examination included the squeezing phenomenon for which we find that the parameter q plays a role of increasing and decreasing the amount of squeezing in each quadrature. Also we examined the second-order correlation function where the system starts with sub-Poissonian behavior in the first mode and then it turns to be super-Poissonian. However, for the second mode the function starts with super-Poissonian and then it turns to show sub-Poissonian for large values of r. Also we managed to deduce the relationship between the linear correlation function and the parameter q from which we can control the amount of the correlation. The nonclassical properties were pronounced when we examined the quasiprobability distribution function. For example, the Wigner function displayed a sharp peak with negative and positive values at the center which depends on the value of the involved parameters. This is reported for both diagonal and off-diagonal cases. The situation was different for the Q-function which shows a Fock-state behavior. However, the effect of the squeeze parameter was still pronounced. The quadrature distribution function is also examined and we find the number of the peaks is always equal to $q + 1$ with a symmetry around the center. Finally we examined phase-distribution function using the Pegg-Barnett formalism in which the state parameter ξ and the squeeze parameter r as well as the q parameter play a crucial role of changing the phase behavior.

Acknowledgement One of us (M.S.A.) is grateful for the partial support from the Research Center, College of Science, King Saud University.

References

1. Agrwal, G.S.: Phys. Rev. Lett. **57**, 827 (1986)
2. Agrwal, G.S.: J. Opt. Soc. Am. B **5**, 1988 (1940)
3. Gou, S.C., Steinbach, J., Knight, P.L.: Phys. Rev. A **54**, 4315 (1996)
4. Obada, A.-S.F., Khalil, E.M.: Opt. Commun. **24**, 1646 (2006)
5. Khalil, E.M., Abdalla, M.S., Obada, A.-S.F.: Ann. Phys. **321**, 421 (2006)
6. Glauber, R.J.: Phys. Rev. **130**, 2529 (1963)
7. Glauber, R.J.: Phys. Rev. **131**, 2766 (1963)
8. Mollow, B.R., Glauber, R.J.: Phys. Rev. **160**, 1097 (1967)
9. Yuen, P.H.: Phys. Rev. A **13**, 2226 (1976)
10. Kim, M.S., de Oliveira, F.A.M., Knight, P.L.: Opt. Commun. **72**, 99 (1989)
11. Kim, M.S., de Oliveira, F.A.M., Knight, P.L.: Phys. Rev. A **40**, 2494 (1989)
12. Paulina, M.: Phys. Rev. A **44**, 3325 (1991)
13. Paulina, M.: Phys. Rev. A **45**, 2044 (1992)
14. EL-Orany, F.A.A., Abdalla, M.S.: A-.S. F. Obada and G.M. Abd Al-Kader. Int. J. Mod. Phys. B **15**, 75 (2001)
15. Abdalla, M.S., Obada, A.-S.F., Darwish, M.: J. Opt. B Quantum Semiclass. Opt. **7**, S695 (2005)

16. Barnett, S.M., Knight, P.L.: J. Mod. Opt. **34**, 841 (1987)
17. Shapiro, J.H., Yuen, H.P., Machado, M.J.A.: IEEE Trans. Inf. Theory IT **25**, 179 (1979)
18. Collett, M.J., Gardiner, C.W.: Phys. Rev. A **30**, 1386 (1984)
19. Collett, M.J., Loudon, R.: J. Opt. Soc. Am. B **4**, 1525 (1987)
20. Caves, C.M., Schumaker, B.L.: Phys. Rev. A **31**, 3068 (1985)
21. Schumaker, B.L., Caves, C.M.: Phys. Rev. A **31**, 3093 (1985)
22. Caves, C.M.: Phys. Rev. D **23**, 1693 (1981)
23. Abdalla, M.S., Obada, A.-S.F., Darwash, M.: Phys. Scr. **77**, 055002 (2008)
24. Abdalla, M.S., Obada, A.-S.F., Darwash, M.: Opt. Commun. **274**, 372 (2007)
25. Nguyen, B.A., Truong, M.D.: J. Opt. B. Quanum Semiclass Opt. **4**, 289 (2002)
26. Pegg, D.T., Barnett, S.M.: Eur. Phys. Lett. **6**, 483 (1988)
27. Barnett, S.M., Pegg, D.T.: J. Mod. Opt. **36**, 7 (1989)
28. Pegg, D.T., Barnett, S.M.: Quantum Opt. **2**, 225 (1997)